

## Liquefaction prevention via floating grid-form deep mixing wall with the auxiliary construction method

Kazuhiro Kaneda<sup>1</sup>, Y. Hirai<sup>1</sup>, S. Tsukuni<sup>2</sup>, and T. Sugano<sup>3</sup>

<sup>1</sup> Takenaka R&D Institute, 1-5-1 Ohtsuka, Inzai, Chiba 270-1395, Japan.

<sup>2</sup> Takenaka Civil Engineering & Construction Co., Co., Ltd., 1-5-1 Ohtsuka, Inzai, Chiba 270-1395, Japan.

<sup>3</sup> Kanto Gakuin University, Research Advancement Management Organization, 1-50-1, Mitsuura Higashi, Kanazawa-ku, Yokohama, 236-8501, Japan.

### ABSTRACT

In recent years, the demand for measures to control the liquefaction in existing harbor structures has increased. However, from the perspectives of constructability and cost, the application of grid-form deep-mixing walls to these types of structures requires the formation of a wider grid spacing compared to conventional designs to prevent liquefaction. The floating grid-form deep mixing wall is proposed to save cost. However, the applicability of wider grid spacing has not yet been studied. In this study, the floating grid-form mixing wall method with auxiliary methods (surface compaction and surface treatment with cement) was investigated for application to the required performance of a structure. In this research, centrifuge model tests were performed. The settlements of the structure and ground liquefaction were focused on. Compared to no-improvement, the floating grid-form mixing wall reduced the subsidence amount by half. It is clear that the effect of settlement reduction of floating grid-form mixing wall. The rise and fall in subsidence was also found to reduce.

**Keywords:** liquefaction; grid-form deep mixing wall; surface improvement

### 1 INTRODUCTION

The requirement for control measures against the liquefaction of existing harbor structures has increased in recent years. It is widely known that the grid-form deep mixing wall (PWRI, 1999; Taya et.al., 2008) was effective in preventing the liquefaction due to the Hyogo-ken Nanbu earthquake and the Tohoku Pacific earthquake (Uchida et al., 2013). Conventionally, the liquefaction layer, as a whole, is improved. As the liquefaction layer thickens, the amount of improved soil increases and the cost rises. Besides, the applicability of the liquefaction layer exceeding 20 m has not been sufficiently verified. On the other hand, due to cost reduction requests, the floating grid-form deep mixing wall was developed, which improved the middle of the liquefaction layer. Although by using this method the amount of improved soil was reduced, the liquefaction later under improved soil could not be prevented.

In a previous research on the floating grid-form deep mixing wall, Takahashi et al. (2012) focused on the grid interval and length of improved soil. The surface settlement and excess pore pressure in soil liquefaction was discussed. However, the structure above the floating grid-form deep mixing wall was not considered.

In this research, liquefaction prevention in a container yard was assumed under a wide grid interval and deep liquefaction layer. After a large earthquake, the design ground motion becomes larger. The design concept is changing from preventing liquefaction to allowing liquefaction according to the required performance (For example, allowable settlement amount) of the structure. The countermeasures that can facilitate early-stage restoration are desired. One of the countermeasures is the floating grid-form deep mixing wall. However, by using the floating grid-form deep mixing wall at a wide grid interval, there is a possibility that the settlement becomes large. Centrifuge model experiments assuming surface compaction and surface treatment with cement inside the grid were carried out as an auxiliary construction method to satisfy the required performance of the structure.

### 2 OUTLINE OF THE CENTRIFUGE MODEL EXPERIMENT

Experiments were performed with the centrifuge model test of Takenaka Corporation. The specifications were as follows: effective radius of 6.5 m, model dimensions of 1.0 m width × 1.0 m depth × 0.5 m height, maximum frequency of 200 Hz, maximum horizontal acceleration of 60g, and maximum centrifugal acceleration of 100g. The tests were performed at a centrifugal acceleration of 50g by using a rigid container having a width of 1100 mm, depth 400 mm, and height 290 mm. In the prototype, the model container dimensions were 88 m (width), 32 m (depth), and

23.28 m (height) (In this study, the prototype values were used.) A container as a structure for carrying packages (width: 2.4 m, depth: 12.2 m, and height: 2.6 m) was modeled as six rows in the horizontal direction and two rows in the vertical direction. The distribution stress of the container was 42.89 kPa. There are two experiments. Case-1 is the non-treatment case and Case-2 is the treatment case using the floating grid-form deep mixing wall from GL-1.5 m to -15 m (wall height: 13.5 m) with a 25 m grid interval. The grid interval is expressed as the horizontal distance between the centers of the grid walls. Figure 1 shows the experimental model with plain and sectional views. The ground level was set at GL-2.8m. The ground from top to GL-20m was made using Iide sand (No.6) with relative density 72%. The maximum ( $e_{max}$ ) and minimum ( $e_{min}$ ) void ratios of Iide sand (No.6) were 0.872 and 0.514, respectively. The stress ratio of single amplitude strain 2.5% at the cycle number 20 was 0.227, obtained using the cyclic triaxial test. The depth of the liquefiable layer was 17.2 m. The ground from GL-20 m to GL-22 m was made using Iide sand (No.6) with relative density 90%, which is dense sand. The ground was made by the falling drop method. As a pore fluid, viscous silicone oil was used in accordance with the similarity law. The silicone oil was poured into soil from the drain gage under the bottom of the container with the vacuum condition. In Case-2, there were two treatments at the surface inside the grid. One was the compaction with Dr 90% using Toyoura sand from the surface to GL-2.8 m, and the other was cement treatment with cement milk (CM=5%, W/C=100%) from GL-1.5 to GL-2.8m. The settlement of the container and ground surface, pore pressure (GL-5m, GL-10m, GL-15m, and GL-20m) and horizontal acceleration (same as pore pressure, surface and top of the container) were measured as shown in figure 1.

Picture 1 shows the situation at the completion of the ground preparation. The model of the floating grid-form deep mixing wall was made of glass epoxy with a width of 0.9 m. The input motion was made by vibration analysis using a site earthquake. Step vibration was adopted with accelerations given in Table 1. Figure 2 shows the acceleration experienced by the shaking table at the third step in Case-1.

### 3 EXPERIMENTAL RESULTS AND DISCUSSION

#### 3.1 Excess pore water pressure

Figure 3 shows the distribution between maximum excess pore-pressure ratio and elevation. A denominator to calculate excess pore-pressure ratio was effective vertical stress  $\sigma_v'$ . In Case-1, liquefaction occurred at the surface soils outside the container (Pa1–4) under the third vibration with a maximum excess pore-pressure ratio of 1.0. Liquefaction did not occur at the center of the container (Pb1–4) with a maximum excess pore-pressure ratio of 0.8.

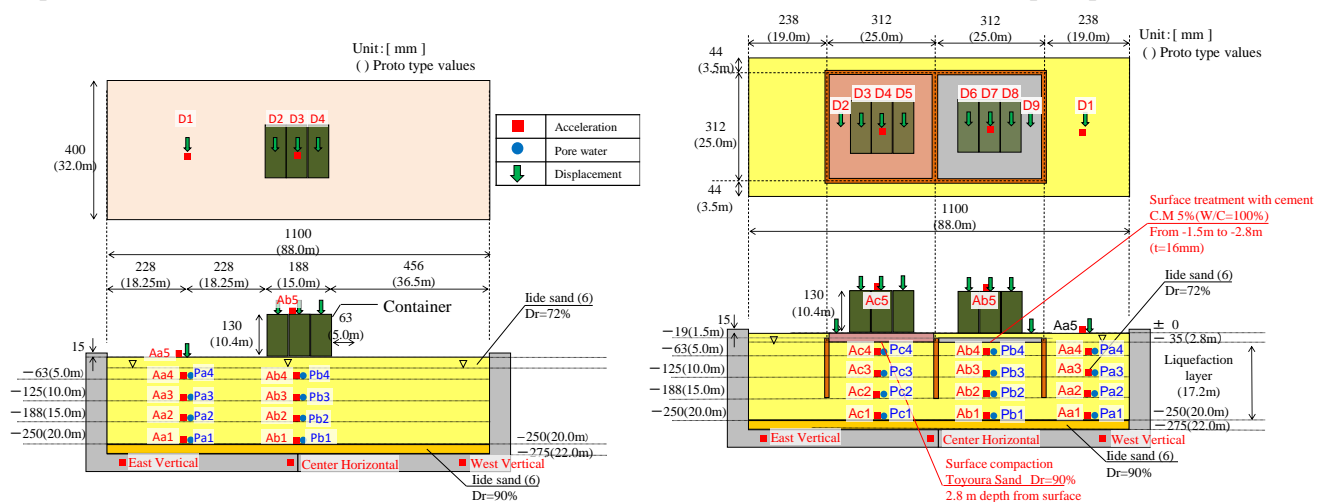


Fig. 1 Experimental model with plain and sectional views.

Table 1 Maximum acceleration.

|            | Case-1 | Case-2 |
|------------|--------|--------|
| 1step(gal) | 111    | 111    |
| 2step(gal) | 149    | 145    |
| 3step(gal) | 271    | 310    |



Pic. 1 Situation at the completion of the ground preparation.

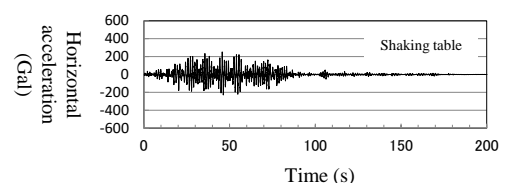


Fig. 2 Acceleration observed by shaking the table at the third.

This is because the weight of the container was summed as the effective vertical stress to calculate the excess pore-pressure ratio. However, from the consideration of acceleration history, liquefaction occurred as described later (figure-5). On the other hand, in Case-2, the maximum excess pore-pressure ratio of both compaction and surface treatment reached 0.9 at GL-15m under the third vibration. However, the rising maximum excess pore-pressure ratio of both compaction and surface treatment was suppressed at GL-5m compared to the non-treated state. It is clear that the liquefaction did not occur with the surface compaction and surface treatment with cement. The maximum excess pore-pressure ratio reached 1.2 at the soils outside the container (Pa1-4) under the third vibration. It is considered that the pore water pressure generated in the grid propagated to the surroundings.

### 3.2 Settlement

Table-2 shows each surface settlement and the final settlement state of the container. In Case-1, the settlements did not occur under the first and second vibrations with small maximum acceleration. It is clear that the maximum excess pore-pressure ratio is small, as seen in figure 3. The surface settlement of the surrounding ground is 309 mm with liquefaction under the third vibration. The container settlement is 572 mm on average. Because the stiffness of the soil under the the container descended, the settlement occurred with the container weight. The difference between the settlement beneath the container and surrounding ground was 260 mm. In Case-2, the surface settlement of the surrounding ground was 161 mm under the third vibration. This is smaller than the corresponding one in Case-1. Because of the use of the rigid container, the space between the rigid container and grid-form deep mixing wall was not so wide, the surrounding surface was not considered a free field. The average settlement (D3, 4, 5) of surface compaction of the container was 198 mm and the difference between this settlement and surface settlement near the container (D2) was 15 mm. This value is very small. Furthermore, the average settlement (D6, 7, 8) with surface

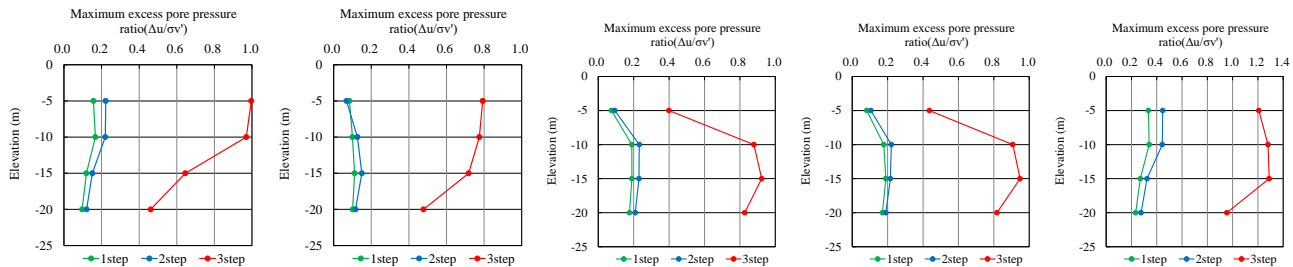
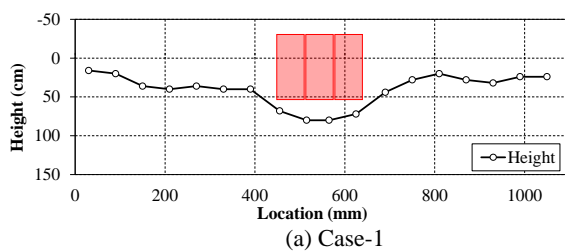


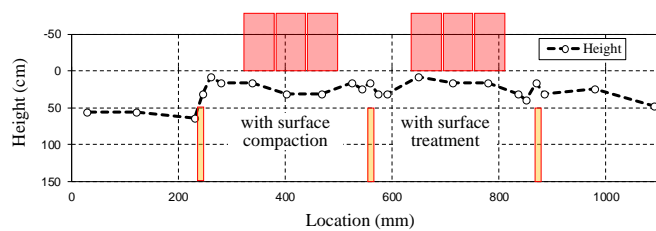
Fig. 3 Distribution between maximum excess pore-pressure ratio and elevation.

Table 2 Each surface settlement and the final settlement state of the container.

|       | Case-1 |     |     |     | Case-2 (Unit:mm) |     |     |     |     |     |     |     |     |
|-------|--------|-----|-----|-----|------------------|-----|-----|-----|-----|-----|-----|-----|-----|
|       | D1     | D2  | D3  | D4  | D1               | D2  | D3  | D4  | D5  | D6  | D7  | D8  | D9  |
| 1step | 7      | 16  | 17  | 20  | 11               | 5   | 12  | 9   | 12  | 12  | 12  | 9   | 4   |
| 2step | 12     | 19  | 19  | 20  | 12               | 8   | 12  | 13  | 13  | 12  | 15  | 9   | 7   |
| 3step | 309    | 515 | 620 | 583 | 161              | 183 | 165 | 239 | 189 | 126 | 179 | 130 | 160 |



(a) Case-1



(b) Case-2

Fig. 4 Final settlement state around a container.

treatment of the container with cement was 145 mm and the difference between this settlement and surface settlement near the container (D9) was 15 mm. This value is also small. It can be concluded that the settlement of the surface treatment with cement is smaller than that of one with surface compaction. Figure 4 shows the final settlement state around a container. It shows the state at the 1 gravity state not 80 G, so the settlement state is a little different from 80 G. In Case-1, the surface settlement occurs at the center of the container; however, in Case-2 the surface settlement both under the container and surrounding ground inside the grid is small and flat. The settlement outside the grid is larger than one inside the grid. It is clear that the settlement was suppressed by improving the surface layer (compaction or treatment with cement) and a difference between the settlement of the container and settlement near the container is small with a 25-m wide space of the grid-form deep mixing wall.

### 3.3 Acceleration

Figure 5 shows the acceleration time histories from 10 s to 60 s on Aa1, Aa4, Ab1, and Ab4 for Case-1, third vibration. The time histories of Aa1 and Ab1 are almost same; however, after 35 s in Aa4 and after 40 s in Ab4, spike-like acceleration histories with cyclic mobility are observed and liquefaction occurs. Although in figure 3 the maximum excess pore-pressure ratio does not reach 1.0, considering the container weight, it can be seen from the acceleration time history that liquefaction occurs. The time difference at which a spike-shaped acceleration history occurs about Aa4 and Ab4 is considered the effect of the constraint pressure on the soil due to the container weight. Figure 6 shows the acceleration time histories from 10 s to 60 s on Ac1, Ac2, Ac3, Ac4, Ab1, Ab2, Ab3, and Ab4 for Case-2, third vibration. The location at Ac2 and Ab2 is the toe of the floating grid-form deep mixing wall and it can be seen that liquefaction occurs after 40 s. Liquefaction also occurred at Ac3 and Ab3. The response of acceleration time histories at Ac4 and Ab4 is small after 40 s because liquefaction occurred at the deeper area and the propagation of waves was small. Figure 7 shows the horizontal displacement time histories obtained by integrating the acceleration from 10 s to 80 s on Aa5 and Ab5 in Case-1 and Ac5 and Ab5 in Case-2, third vibration. In Case-1, the motions of the surrounding ground (Aa5) and the container (Ab5) coincide well up to 45 s; however, after 45 s, the horizontal displacements of the container occur frequently. From the acceleration time history (Ab4) in figure 5 around 45 s, the large amplitude of cyclic mobility cannot be seen. In other words, that soil was liquefied and there is a time of relative small stiffness of soils. Acceleration is not transmitted until the soil stiffness is restored. This effect is considered to have increased the deformation of the upper container. On the other hand, in Case-2, it is clear that the responses of Aa5 and Ab5 are almost same and the horizontal deformation is smaller than that in Case-1.

### 4 CONCLUSION

The countermeasure to liquefaction was analyzed using centrifuge model tests. It was concluded that relative settlements (difference between the settlement of the container and surrounding surface settlement) were suppressed to less than half compared to non-treatment soil using surface compaction or surface treatment with cement, even with a wide grid interval of 25 m. It was found that liquefaction occurred in soils under floating grid-form deep mixing walls and the waves transmitted to the upper part and the surface layer inside the grid were attenuated under its influence. It is clear that horizontal displacement can occur largely due to the influence of liquefaction on the surface of the structure (container) in the non-treatment case. However, the horizontal displacement can be suppressed by the improved floating grid-form deep mixing wall.

### REFERENCES

- The Ministry of Construction public works research institute (PWRI) (1999). Liquefaction counter measure technical method manual of design and construction (plan). Joint Study Report, 486, 478.
- Taya, Y., Uchida, A., Yoshizawa, M., Onimaru, S., Yamashita, K., and Tsukuni, S. (2008). Simple method for determining lattice intervals in grid-form ground improvement. Japanese Geotechnical Journal, 3(3), 203-212.
- Uchida, A., Odajima, N. and Yamashita, K. (2013). Performance of building foundation with grid-form ground improvement during the 2011 Tohoku Pacific Earthquake. AIJ Journal of Technology and design, Des, 19(42), 481-484.
- Takahashi, H., Morikawa, Y., Tsukuni, S., Yoshida, M. and Hisada, H. (2012). Approach to reducing improvement depth of

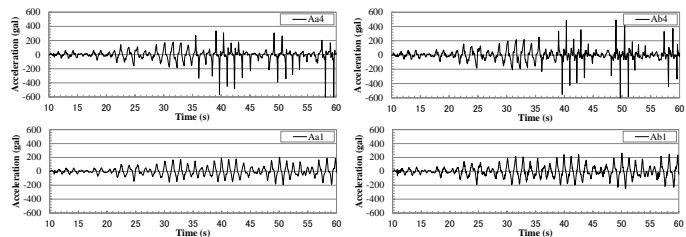


Fig. 5 Acceleration time histories (Aa1, Aa4, Ab1, and Ab4, Case-1, third vibration).

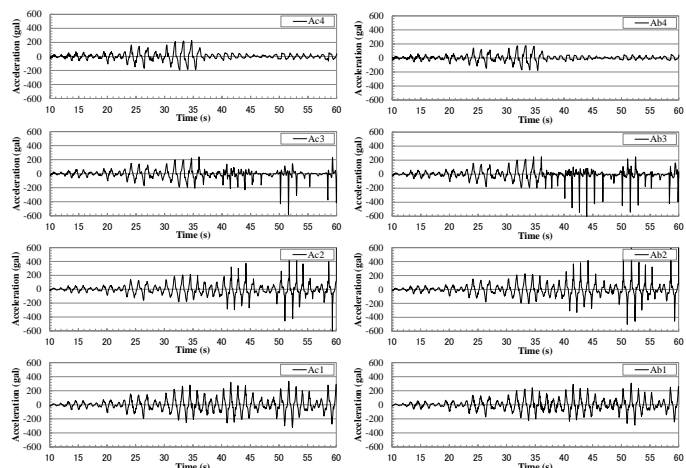
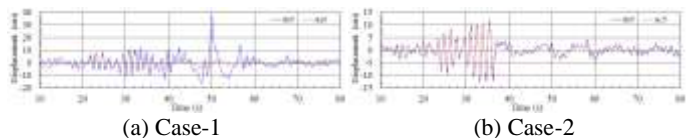


Fig. 6 Acceleration time histories (Ac1, Ac2, Ac3, Ac4, Ab1, Ab2, Ab3, and Ab4, Case-2, third vibration).



(a) Case-1 (b) Case-2  
Fig. 7 Horizontal displacement time histories (Aa5 and Ab5 in Case-1 and Ac5 and Ab5 in Case-2, third vibration.).

lattice-shaped cement treatment method for liquefaction countermeasure. Report of the Port and Airport Research Institute, 51(2), 3-39.